GROUND TRUTH, MAGNITUDE CALIBRATION AND REGIONAL PHASE PROPAGATION AND DETECTION IN THE MIDDLE EAST AND HORN OF AFRICA

Andrew A. Nyblade[1], Aubreya Adams[1], Richard A. Brazier[1], Yongcheol Park[1], and Arthur Rodgers[2]

Penn State University[1] and Lawrence Livermore National Laboratory[2]

Sponsored by National Nuclear Security Administration
Office of Nonproliferation Research and Development
Office of Defense Nuclear Nonproliferation

Contract Nos. DE-FC52-05NA26602[1] and W-7405-ENG-48[2]

ABSTRACT

In this project, we are exploiting unique and open source seismic data sets to improve seismic monitoring across the Middle East (including the Iranian Plateau, Zagros Mountains, Arabian Peninsula, Turkish Plateau, Gulf of Aqaba, Dead Sea Rift) and the Horn of Africa (including the northern part of the East African Rift, Afar Depression, southern Red Sea and Gulf of Aden). The data sets are being used to perform three related tasks. 1) We are determining moment tensors, moment magnitudes and source depths for regional events in the magnitude 3.0 to 6.0 range. 2) These events are being used to characterize high-frequency (0.5-16 Hz) regional phase attenuation and detection thresholds, especially from events in Iran recorded at stations across the Arabian Peninsula. 3) We are collecting location ground truth at GT5 (local) and GT20 (regional) levels for seismic events with M > 2.5, including source geometry information and source depths.

In the first phase of this project, seismograms from earthquakes in the Zagros Mountains recorded at regional distances have been inverted for moment tensors, and source depths for the earthquakes have been determined via waveform matching. Early studies of the distribution of seismicity in the Zagros region found evidence for earthquakes in the upper mantle. But subsequent relocations of teleseismic earthquakes suggest that source depths are generally much shallower, lying mainly within the upper crust. Nine events with magnitudes between 5 and 6 have been studied so far. Source depths for six of the events are within the upper crust, and three are located within the lower crust. The uncertainty in the source depths of the lower crustal events allows for the possibility that some of them may have even nucleated within the upper mantle. Eight events have thrust mechanisms and one has a strike-slip mechanism.

We also report estimates of three-dimensional P- and S-wave velocity structure of the upper mantle beneath the Arabian Peninsula obtained from travel time tomography. Travel time measurements were obtained using a data set provided by King Abdulaziz City for Science and Technology (KACST) for the Saudi Arabia National Digital Seismic Network. The network consists of 38 stations (27 broadband and 11 short period). We augmented the KACST data with delay times measured from permanent stations in the region and the 1995-7 Saudi Arabian PASSCAL Experiment. Tomographic images reveal a low velocity feature in the upper mantle stretching north-south beneath the central portion of the Arabian Shield.

OBJECTIVES

The objective of this effort is to determine ground truth source parameters (depth, moment, focal mechanism) for earthquakes in the Middle East. For this reporting period we focused on events in the Zagros Mountains of Iran using unique broadband waveforms from regional stations. Source moments will be used to calibrate coda wave moment magnitudes (Mayeda et al., 2003) and to model high-frequency regional body-wave amplitude spectra with the Magnitude-Distance Amplitude Correction (MDAC) methodology (Walter and Taylor, 2002). In subsequent periods, we will determine models of the propagation characteristics, including attenuation, of high-frequency regional phases. These models will then be used to estimate detection thresholds by comparing model-based predictions of signal amplitudes to background noise levels.

RESEARCH ACCOMPLISHED

Introduction

In this project, we are exploiting unique and open source seismic data sets to improve seismic monitoring for the Middle East (including the Iranian Plateau, Zagros Mountains, Arabian Peninsula, Turkish Plateau, Gulf of Aqaba, and Dead Sea Rift) and the Horn of Africa (including the northern part of the East African Rift, Afar Depression, southern Red Sea, and Gulf of Aden). Broadband waveform data sets are being used to perform three related tasks. 1) We are determining moment tensors, moment magnitudes and source depths for regional events in the magnitude 3.0 to 5.0 range. 2) These events are being used to characterize high-frequency (0.5-16 Hz) regional phase attenuation and detection thresholds, especially from events in Iran recorded at stations across the Arabian Peninsula. 3) We are collecting location ground truth at GT5 (local) and GT20 (regional) levels for seismic events with M > 2.5, including source geometry information and source depths.

The results of this research will enhance monitoring capabilities within the study region by improving our understanding of high frequency regional phase attenuation and how this attenuation affects detection thresholds. Accurate hypocentral locations of M>2.5 seismic events are needed to construct travel time correction surfaces, which are of fundamental importance to ground-based nuclear explosion monitoring.

The work completed so far in this project has focused on obtaining well constrained source parameters for magnitude 5.0 and greater events in the Zagros Mountains of Iran that have been well recorded at regional distances. Focal mechanisms have been obtained through standard moment tensor inversion of regional waveforms, and a grid search procedure has been applied to find the source depth that produces the best fit to the regional waveforms. As part of this project, we have also imaged three-dimensional P- and S-wave velocity structure of the upper mantle beneath the Arabian Peninsula using teleseismic travel time tomography. We have completed travel time measurements and inversion for a data set provided by KACST for the Saudi Arabia National Digital Seismic Network. The network consists of 38 stations (27 broadband and 11 short period). We augmented the KACST data with delay times measured from permanent (GNS/IMS) stations in the region (RAYN, EIL and MRNI) and the 1995-7 Saudi Arabian PASSCAL Experiment (Vernon and Berger, 1998).

Background

The Arabian Shield consists of late Proterozoic crystalline basement overlain by Tertiary and Quaternary volcanic rocks in some places. The break-up of the Arabian Plate from Africa initiated at about 30-35 million years ago (Ma), with the formation of the Red Sea-Gulf of Aden rift system (Coleman and McGuire, 1988). Volcanism was widespread between 30 and 12 Ma, and uplift of the Arabian Shield occurred at about 13 Ma (Coleman and McGuire, 1988). The volcanism and uplift are thought to be related to the presence of hot upper mantle (Camp and Roobol, 1992). The uplifted Arabian Shield contains two major features: one is the
Makkah-Madinah-Nafud (MMN) volcanic line in the south and the other is the Ha'il-Rutbah Arch in the north (Figure 1). The MMN volcanic line, extending north-south, has been the major site of volcanism in Saudi Arabia over the past 10 Ma and the Ha'il-Rutbah Arch has been the site of several periods of uplift (Camp and Roobol, 1992).

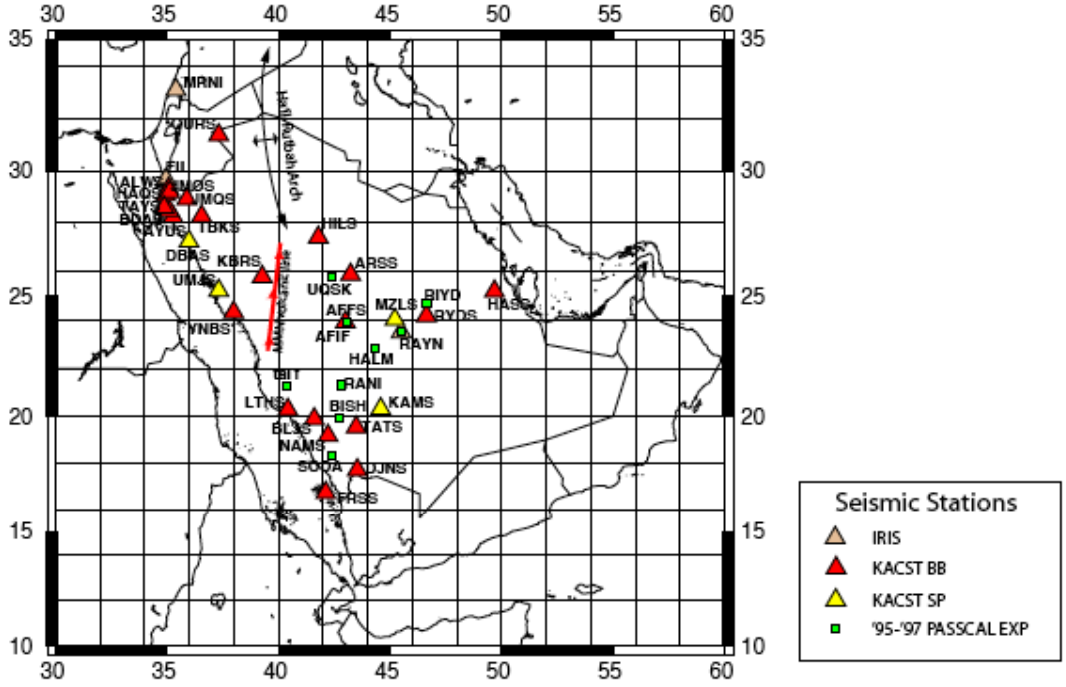

Figure 1. Map showing seismic stations in the Arabian Peninsula used in this study. KACST stations belong to the Saudi Arabia Digital National Seismic network.

The Zagros Mountain Belt, one of the world's most seismically active mountain ranges, marks the convergent boundary between the Arabian and Eurasian plates in southwestern Iran (Figure 2). The upper 11 km of the crust consists of folded sedimentary layers, while the lower 36 km of the crust are composed of faulted crystalline basement rock. The most prominent fault exposed at the surface is the Zagros Main Thrust, which marks the northern extent of seismicity associated with the Zagros Mountains and separates the Zagros Mountains from the Central Iranian Plateau. The Moho dips to the northeast from a depth of 40 km beneath the Persian Gulf to a maximum depth of approximately 65-70 km beneath the Zagros Main Thrust (Paul et al., 2006). Early studies of the distribution of seismicity in the Zagros region found evidence for earthquakes in the upper mantle (Nowroozi, 1971; Bird et al., 1975). Subsequent recalculations of teleseismic earthquakes indicated that source depths were much shallower, lying within the upper crust (Maggi et al., 2000, 2002).

Figure 2. Colored topography map of the Middle East showing the location of the main plates and the Zagros Mountains.

Zagros Earthquakes

Source depths and focal mechanisms for nine new events have been obtained (Table 1). A grid search method was used to determine the source parameters of each event. First, regional waveforms for each event were inverted for a moment tensor over a range of potential source depths. Synthetic seismograms were then computed using a reflectivity code for each source mechanism and compared to observed waveforms. In addition to the KACST and PASSCAL stations, data recorded at regional distances on open stations to the north and east were used, providing fairly good azimuth ray coverage for each event. The quality of the visual fit between the synthetic and observed waveforms, along with the root mean square error, were used to determine the best-fitting focal mechanism and associated source depth.

The locations of the events are shown in Figure 3. Most of the events studied occurred within the central portion of the Zagros Mountains where there are the best constraints on crustal structure provided by receiver function and gravity studies. Figure 4 summarizes graphically the results for the nine events, and shows a selection of the waveform fits for each event. Eight events have thrust mechanisms and one has a strike-slip mechanism. Source depths for six of the events are within the upper crust, and three are located within the lower crust. The uncertainty in the source depths of the lower crustal events allows for the possibility that some of them may have even nucleated within the upper mantle. The depth distribution of the events with uncertainties is shown in Figure 5.

Table 1a. Source parameters for events in the Zagros Mountains. Event letters are the same as in Figure 3.

Event Letter	Event ID Number	Date MM/DD/YYYY	Time	M0	Mw	Mw CMT	Strike/Dip/Rake (Plane 1)	Strike/Dip/Rake (plane 2)
A	9962	11/13/1998	13:01:10	1.35E+24	5.4	5.4	144.21/65.33/120.95	269.05/38.80/41.76
B	1320614	10/31/1999	15:09:40	7.13E+23	5.2	5.2	158.09/69.17/102.39	306.38/24.10/60.58
C	776913	05/06/1999	23:00:53	5.44E+26	7.1	6.2	19.15/10.66/-6.79	115.83/88.75/259.41
D	9816	10/05/1998	02:20:36	1.26E+24	5.4	5.4	40.91/85.77/206.56	308.80/63.51/-4.73
E	4070289	03/01/2000	20:06:29	1.93E+23	4.8	5.0	298.57/49.98/134.73	61.56/57.04/50.03
F	1326382	03/01/2000	20:06:28	1.78E+23	4.8	5.1	112.26/33.89/122.73	254.50/62.03/70.04
G	1582024	02/17/2002	13:03:53	1.01E+24	5.3	5.5	109.24/10.24/76.99	302.46/80.03/92.33
H	4357281	07/10/2003	17:40:16	4.64E+24	5.7	5.6	343.19/6.42/35.13	218.22/86.31/95.26
I	1559906	04/13/2001	01:04:27	3.93E+23	5	5.1	96.81/14.85/134.62	231.21/79.49/79.45

Table 1b. Moment tensors and source depth for events in the Zagros Mountains. Event letters are the same as in Figure 3.

Event Letter	Mxx	Mxy	Mxz	Myy	Myz	Mzz	Depth
A	8.67E+10	3.73E+10	-4.49E+09	5.16E+09	-9.42E+10	-9.19E+10	12 (+-2)
B	2.35E+10	1.97E+10	-1.13E+10	2.72E+10	-5.13E+10	-5.08E+10	12 (+-2)
C	9.18E+12	1.99E+12	4.85E+13	-1.84E+13	1.86E+13	9.25E+12	54 (+15/-8)
D	-1.18E+11	2.13E+10	3.33E+10	1.04E+11	-4.42E+10	1.35E+10	35 (+15/-5)
E	1.79E+10	2.01E+08	-1.97E+09	-4.28E+09	1.04E+10	-1.36E+10	9 (+-3)
F	1.66E+10	7.22E+08	8.33E+09	-3.64E+09	-4.28E+09	-1.30E+10	9 (+-3)
G	2.85E+10	1.84E+10	7.94E+10	2.29E+09	5.09E+10	-3.08E+10	4 (+-2)
H	4.01E+08	1.31E+10	2.90E+11	8.04E+10	-3.54E+11	-8.08E+10	39 (+10/- 15)
I	1.52E+10	5.69E+08	2.55E+10	2.08E+09	-2.50E+10	-1.73E+10	8 (+-3)

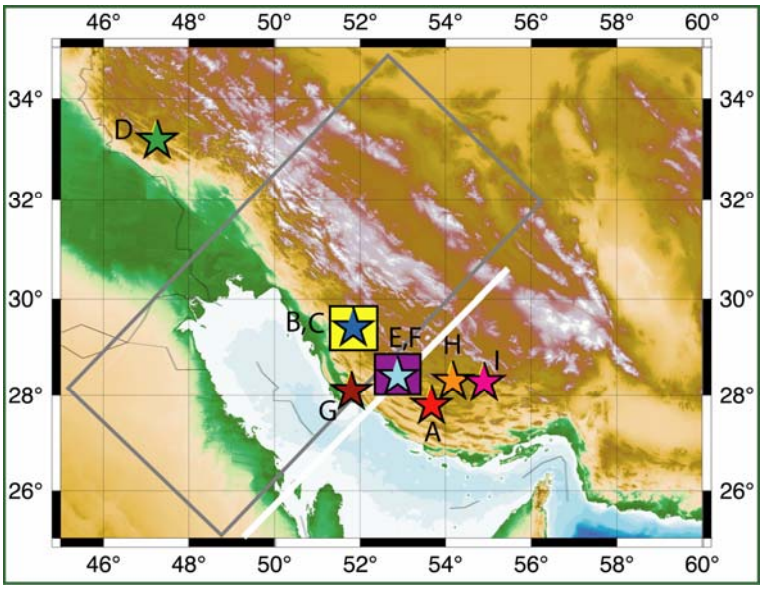

Figure 3. Map of Zagros Mountains and Persian Gulf showing the locations of earthquakes studied. Letters correspond to the events in Table 1. The grey box shows the area where crustal thickness has been constrained using gravity data and the white line shows where crustal thickness has been imaged using receiver functions.

The focal depth of earthquakes can affect the excitation of regional phases, particularly the guided Lg phase, which is composed of higher mode surfaces waves whose amplitudes are strongly depth dependent. The source parameters determined above can be used to infer how focal mechanism and depth might impact regional phase S-wave generation and how this might in turn impact P/S discriminants. Two nearby events (A & H) were recorded at station HILS on the northern Arabian Shield. These events had similar magnitudes (5.4 versus 5.7) and although both are thrust mechanisms their strikes are slightly different. These events have significantly different depths with event A in the upper crust and event H in the lower crust (or upper mantle, but less likely). The high-frequency (0.5-5 Hz) responses of these events are shown in Figure 6. Note that Lg is weaker with respect to the Pn for the deeper event (H), making the Pn/Lg ratio discriminant more explosion-like for this event. This suggests a possible depth-dependence of the Lg amplitude (and Pn/Lg ratio discriminant). Alternatively, the further event (H) may be located in a region of thicker crust, which leads to disruption of the crustal waveguide along the path to HILS. Both explanations would cause additional scatter in body-wave discriminants, compounding discrimination strategies. These observations will be explored in further work on this project.

Body Wave Tomography

Upper mantle structure strongly impacts the propagation of regional Pn and Sn phases. We report velocity structure of the upper mantle reported from teleseismic P- and S-body waves. While this study elucidates deep upper mantle structure, there are likely relationships with structure directly below the crust. To investigate upper mantle structure under the Arabian Shield, we measured and inverted relative travel times from stations across the Arabian Peninsula. We augmented the KACST data with delay times measured from permanent stations in the region (RAYN, EIL and MRNI) and the 1995-7 Saudi Arabian PASSCAL Experiment data set. Figure 1 shows the locations of seismic stations used in this study. We computed travel time differences for two nearly co-located stations (AFFS and AFIF in Figure 1) between KACST and the PASSCAL networks in order to investigate possible biases between these data sets before combining all delay times from different seismic networks. We sorted events recorded on the common stations by back azimuth and distance and measured P-wave travel time residuals from arrival times subtracted from a theoretical travel time. The trends of the residuals with back-azimuth and distance are very similar and indicate no bias between the travel time residuals for the common stations.

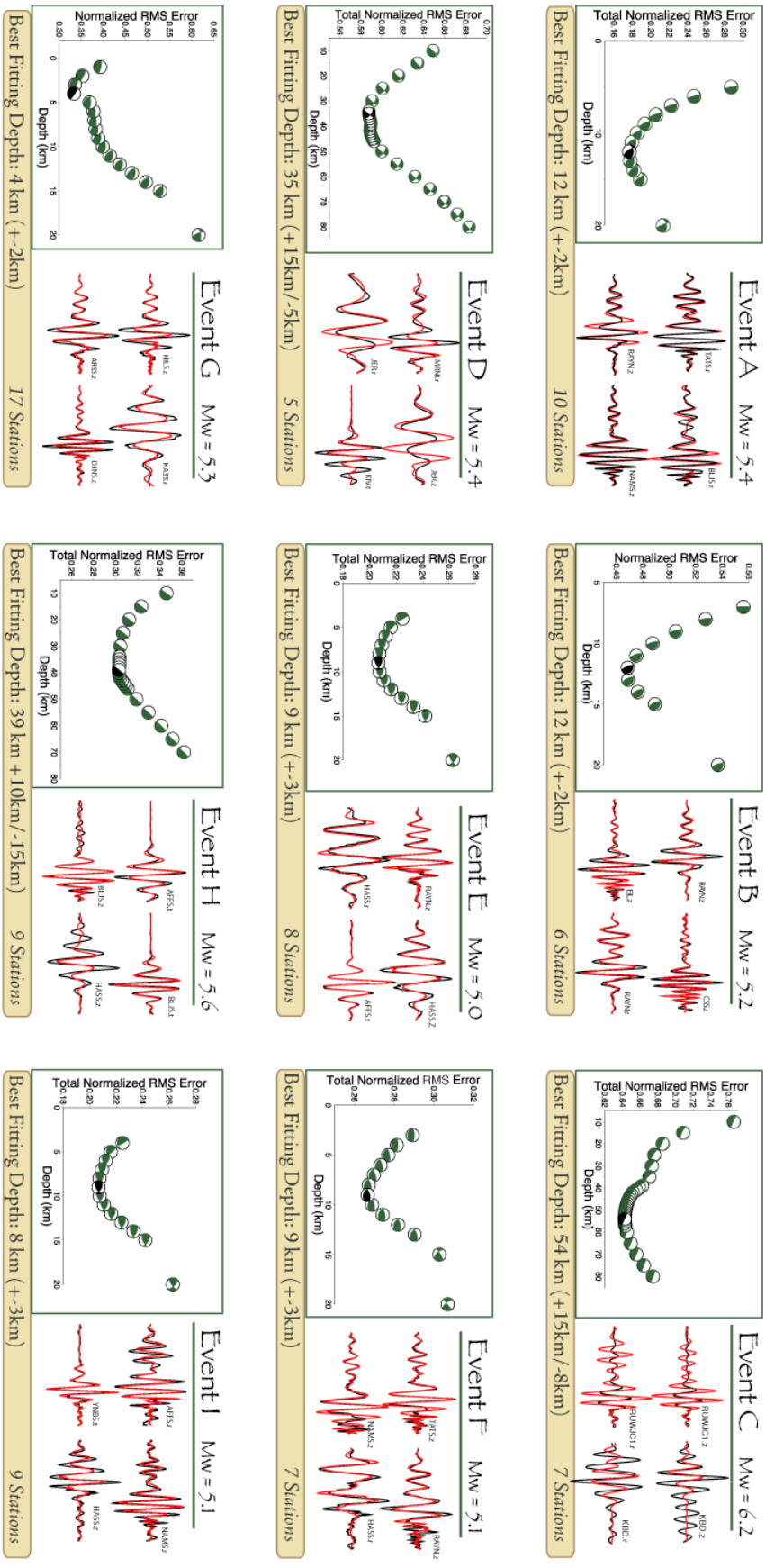

Figure 4. Results from moment tensor inversion and grid search of source depth for nine events studied in the Zagros Mountains. For each event, the graph to the left shows focal mechanism as a function of source depth plotted against RMS error. The focal mechanism and source depth that yields the best fitting synthetics to the data is noted with the black beach ball. Selected waveforms are shown on the right side of each panel. Observed waveforms are in black and synthetics are in red. Event letters are the same as in Table 1 and Figure 3.

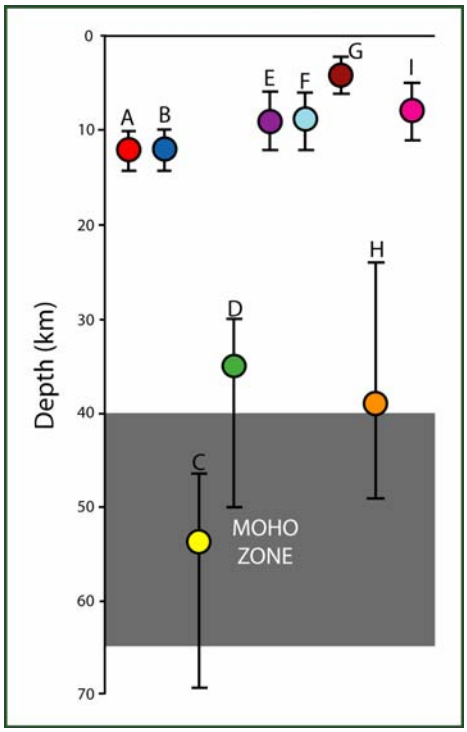

Figure 5. Plot showing source depths for the nine events studied from the Zagros Mountains. Error bars correspond to the uncertainties given in Figure 4. The "Moho Zone" represents the range of Moho depths across the Zagros Mountains within proximity of the earthquakes, as reported from gravity and receiver function studies. Event letters are the same as in Table 1 and Figures 3 and 4.

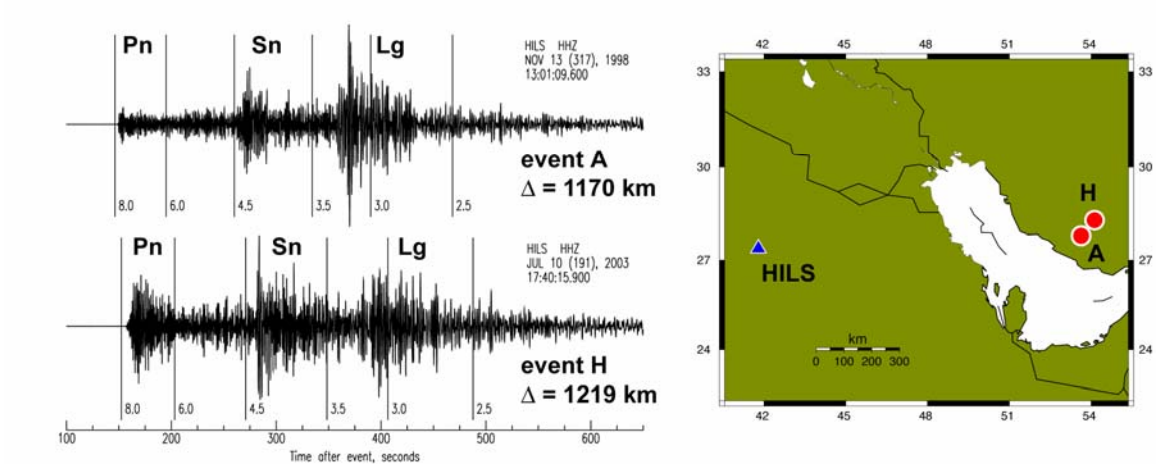

Figure 6. (left) Vertical component waveforms (filtered 0.5-5 Hz) for events A (top) and H (bottom) at station HILS (Al Hail, Saudi Arabia). (right) These events are closely located with event H slightly further away.

For the data sets, we computed relative arrival time residuals using a multi-channel cross-correlation (MCCC) method and inverted for a three dimensional velocity model using the method of VanDecar (1991). For the inversion, we parameterized travel time slowness using a grid of knots comprised of 34 knots in depth, 56 knots latitude between 12.0° N and 37.0° N and 56 knots in longitude between 29.5° E and 55.0° E. The horizontal knot spacing is one third of a degree, and the vertical knot spacing is 25 km in

the inner region of seismic array (17.4° N-30.7° N, 35.5° E-48.5° E, and 0-200 km depth). We used the IASPEI91 model (Kennett and Engdahl, 1991) as the initial model for the inversion.

Results for the P-wave Tomography

We used 401 earthquakes resulting in 3,416 ray paths with P- and PKP-wave arrivals. The majority of the events are located in the western Pacific Rim between back azimuths of 15 and 150 degrees, but the events are distributed over a wide range of back azimuths. The waveforms were filtered with a zero-phase two-pole Butterworth filter between 0.5 to 2 Hz before the relative travel-time residuals were computed. The MCCC procedure was performed over a three-second window on the filtered data. A final model was selected by investigating the way in which changes in regularization levels (flattening and smoothing values) affect the reduction in travel time residuals. To determine a preferred model, 2,000 iterations of the conjugate gradient procedure are performed with several different pairs of flattening and smoothing values. For our preferred model, we have chosen a model with the values of 1,600 for flattening and 3,200 for smoothing.

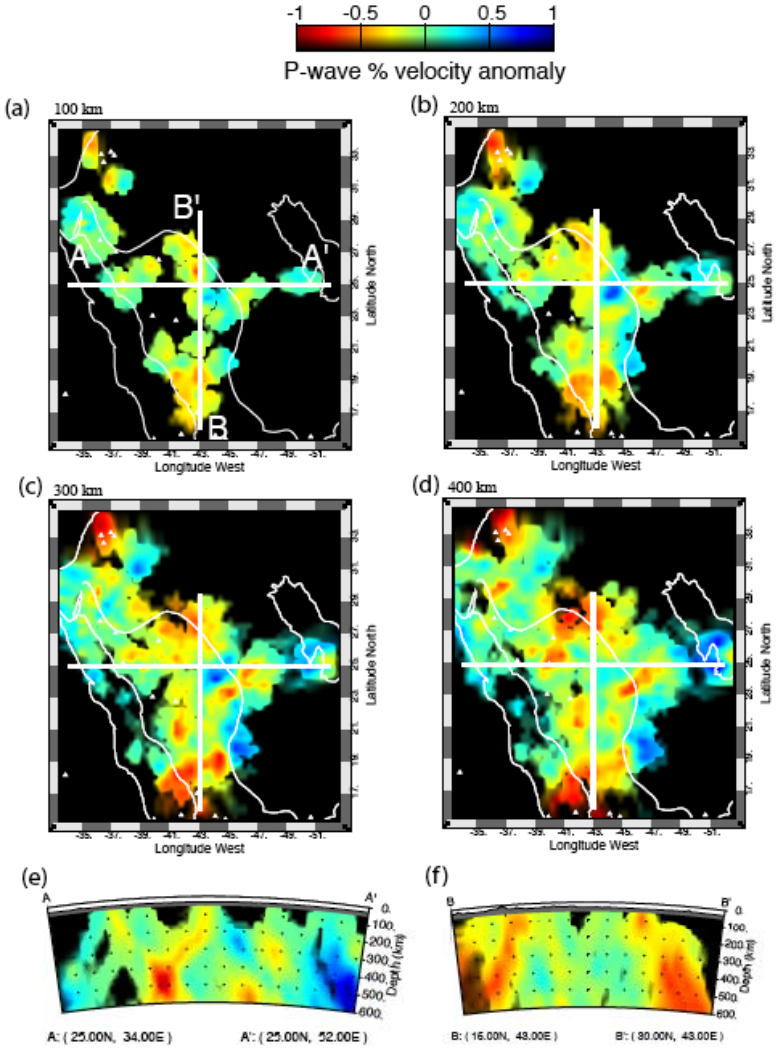

Figure 7. Results of P wave tomography. (a–d) Depth slices through the model at depths of 100, 200, 300 and 400 km. (e-f) vertical slices through the model along E-W (e) and N-S (f) profiles denoted with white lines in a–d.

Figure 7 shows depth slices (a-d) and vertical cross-sections (e and f) through the model. A preliminary interpretation of these features would suggest that low velocities beneath the Gulf of Aqaba and southern

Arabian Shield and Red Sea are related to mantle upwelling and seafloor spreading. Low velocities beneath the northern Arabian Shield may be related to volcanic centers. The origins of the low velocity features near the eastern edge of the Arabian Shield and western edge of the Arabian Platform are unknown.

Results from the S-wave Tomography

For the S-wave model, we used 201 earthquakes resulting in 1,602 ray paths with S- and SKS-wave arrivals. Although the total number of rays for the S-wave model is half of the rays for the P-wave model, the event distribution shows better coverage of back azimuth. The signal processing procedures for the S-wave data are exactly the same as for the P-wave data, but traces were filtered over a lower frequency band (0.04 to 0.1 Hz), and relative arrival time residuals were computed by the MCCC method using a fifteen-second window. As a result we could use the short-period stations for the P-wave analysis, but were limited to data from the broadband stations for the S wave model. The first order velocity variations seen in the S model are similar to the P model, and therefore we do not show the S wave model here.

CONCLUSION(S) AND RECOMMENDATIONS

We reported progress on the determination of ground truth source parameters (focal depths and mechanisms, seismic moments) for earthquakes in the Zagros Mountains. These moments can be used to calibrate coda wave magnitudes and to model high frequency regional phase amplitude spectra with the MDAC methodology. We will explore the effect of location and focal depth on regional phase amplitudes and discriminants and estimate propagation properties (including attenuation, quality factors). Regional phase propagation models (derived from the MDAC methodology) will be developed to improve understanding of high frequency body-wave discriminants and amplitude detection thresholds in the Middle East.

ACKNOWLEDGEMENTS

The facilities of the IRIS Data Management System, and specifically the Incorporated Research Institutions for Seismology (IRIS) Data Management Center (DMS), were used for access to waveform and metadata required in this study. The IRIS DMS is funded through the National Science Foundation and specifically the GEO Directorate through the Instrumentation and Facilities Program of the National Science Foundation under Cooperative Agreement EAR-0004370.

REFERENCES

Bird, P., M. N. Toksoz, and N. H. Sleep (1975). Thermal and mechanical models of continent-continentconvergence zones, *J. Geophys. Res*. 80: 4405–4416.

Camp, V. E., and M. J. Roobol (1992). Upwelling asthenosphere beneath western Arabia and its regional implications, *J. Geophys. Res.* 97: 15255–15271.

Coleman, R. G., and A. V. McGuire (1988). Magma Systems Related To The Red-Sea Opening, *Tectonophysics*, 150: 77–100.

Crosson, R. S. (1990). Determination of teleseismic relative phase arrival times using multi-channel cross correlation and least-squares, *Bull. Seism. Soc. Am.* 80: 150–169.

Kennett, B. and E. R. Engdahl (1991). Travel times for global earthquake location and phase identification, *Geophys. J. Int.* 105: 429–465.

Maggi, A., J. Jackson, K. Priestley and C. Baker (2000). A re-assessment of focal depth distributions insouthern Iran, the Tien Sha and northern India: do earthquakes really occur in the continentalmantle?, *Geophys. J. Int.* 143: 629–661.

Maggi, A., K. Priestley and J. Jackson (2002). Focal depths of moderate to large earthquakes in Iran. *Journal of Seismology and Earthquake Engineering* 4: 1–10.

Mayeda, K., A. Hofstetter, J. O'Boyle and W. Walter (2003). Stable and transportable regional magnitudes based on coda-derived moment-rate spectra, *Bull. Seism. Soc. Am.*, 93, 224–239.

Nowroozi, A. A. (1971). Seismotectonics of the Persian Plateau Eastern Turkey, Caucasus, and Hindu-Kush Regions, *Bull. Seism. Soc. Am*. 61: 317–342.

Paul, A., A. Kaviani, D. Hatzfeld, J. Vergne and Mohammad Moktari (2006). Seismological evidence forcrustal scale thrusting in the Zagros mountain belt, submitted to *Geophys. J. Int.*

VanDecar, J. C. (1991). Upper mantle structure of the Cascadia subduction zone from non-linear teleseismic travel time inversion, Ph. D. Thesis, Univ. of Washington, Seattle, WA.

Vernon, F., and J. Berger (1998). Broadband seismic characterization of the Arabian Shield, Final Scientific Technical Report, Department of Energy Contract No. F 19628-95-K-0015, 36 pp.

Walter, W. and S. Taylor (2002). A revised magnitude and distance amplitude correction (MDAC2)procedure for regional seismic discriminants, Lawrence Livermore National Laboratory technicalreport UCRL-ID-146882.